Study of Dielectric and Piezoelectric Properties of (1-x)PZT-xSFN Ceramics Prepared by Conventional Solid State Reaction Method

[1,2]Fares Kahoul*, [1,2]Louanes Hamzioui, [1]Abderrezak Guemache, [3,4]Michel Aillerie and [2]Ahmed Boutarfaia
[1]*Université de M'Sila, Département Socle Commun ST, Faculté de Technologie, M'Sila 28000 Algérie*
[2]*Université de Biskra, Département de Chimie, Laboratoire de Chimie Appliquée, B. P. 145, RB-Biskra 07000 Algérie.*
[3] *Université de Lorraine, LMOPS, EA 4423, 57070 Metz, France.*
[4]*Centrale Supelec, LMOPS, 57070 Metz, France.*
Fares.kahoul@univ-msila.dz; Fares_260@yahoo.fr*

(Received on 1st April 2019, accepted in revised form 17th Feb 2020)

Summary: Modified-PZT ceramics with a formula (1-x)Pb($Zr_{0.53}$ $Ti_{0.47}$)O_3-xSr($Fe_{2/3}$, $Nb_{1/3}$)O_3 (doped with isovalent: Sr^{2+}, acceptor: Fe^{3+} and Donor: Nb^{5+} ions) abbreviated as (1-x)PZT-xSFN binary system with varying x (x= 0.02, 0.04, 0.06, 0.08 and 0.10) located near the morphotropic phase boundary (MPB) were prepared by a traditional process in a solid state. All the samples were sintered at a temperature of 1200°C during 2 h. The phase structure, the dielectric and piezoelectric properties of the system were studied. In-phase analysis used X-ray diffraction (XRD) at room temperature indicated that the structure of phase of sintered PZT-SFN ceramics was formed in single-phase with a crystalline structure tetragonal. Raman spectroscopy confirms the presence of this tetragonal phase. The optimum electrical parameters are obtained at 0.94Pb($Zr_{0.53}Ti_{0.47}$)O_3-0.06Sr($Fe_{2/3}$, $Nb_{1/3}$)O_3 system: k_p= 66.10 %, d_{31}= 145 pC/N, Q_m= 473, tanδ= 1.11 %, and ε_r= 1009.

Keywords: PZT, Perovskites, XRD, Dielectric properties, MPB.

Introduction

Among the ferroelectric materials that are widely studied is lead zirconate titanate (PZT), because of their area of application as a piezoelectric material. The electromechanical properties of the PZT generated a very high coupling coefficient. A phase diagram of the PZT shows that to the molar report/ratio, the values of the $PbTiO_3$ fractions ranging between 0,4 and 0,6 present a morphotropic phase boundary (MPB) [1–3], who was related to the homogeneity of the composition and the adjustment of the treatment of the sample [3–5]. The PZT prepared starting from materials ferroelectric drew the attention because of their application in the devices of memory, the sensors, the electro-optical devices, etc. [2, 6–9]. It is well-known that the performances of PZT ceramics depend strictly on their structural and microstructural properties, which can be adapted by controlling the parameters of treatment in specific compositions [9, 10].

During last years, the materials aroused a lively interest, which testifies to the characteristic of the MPB. The compositions which belong of MPB are appropriate perfectly for the design and the applications of devices in order to answer the changes of technological revaluation. In order to improve the properties of PZT ceramics according to the needs, a doping is carried out on the PZT in the vicinity of the MPB. Ragini *et al*. [11] gave again that the rhombohedral phase undergoes a transition from anti-ferrodistortive phase in another monoclinical phase with a constant of network doubled in the direction (001). These researchers [12] also carried out the analysis of Rietveld on pure PZT and indicated that the structure is tetragonal (space group P4mm) for X = 0,515, whereas for X = 0,520 and 0,525, the phases tetragonal and rhombohedral (space group Cm) to coexist.

The general formula of PZT is ABO_3 of the perovskite structure, in which the site A is occupied by Pb^{2+}, and the site B is occupied at the same time by Zr^{4+} and Ti^{4+}. The perovskite structure can be doped at both sites A and B with various ions, for the purpose of improving the properties of the material. The doping of the perovskite structure depends only on the size of the sites and it is independent of the acceptor and donor properties of the foreign ions. The structural and electrical properties of the doped PZT are strongly related to the presence of defects after the doping phenomenon [13, 14]. The deformation due to size reduction, surface effects and structure distortion are governed directly on the electrical properties (remnant polarization, Curie transition temperature and dielectric constant) of the material.

To our knowledge, the properties of (1-x)PZT-xSFN ceramics has not been investigated before. This research is based on the development of a new ceramic material of binary system (1-x) PZT-xSFN, near the

*To whom all correspondence should be addressed.

MPB region which should present excellent piezoelectric properties. The evolution of the density, the phase and the dielectric and piezoelectric properties according to the molar fraction of SFN on PZT ceramics was studied and discussed.

Experimental

The method of elaboration of the ceramic samples is ensured by a sintering process, with these compositions: (1-x)Pb($Zr_{0.53}$ $Ti_{0.47}$)O_3-xSr($Fe_{2/3}$, $Nb_{1/3}$)O_3 denoted (1-x)PZT-xSFN (x = 0.02, 0.04, 0.06, 0.08 and 0.10). The oxides, Pb_3O_4, ZrO_2, TiO_2, $SrCO_3$, Nb_2O_5, and Fe_2O_3, are dried beforehand in an oven for 24 h at 75 °C and are then ball-milled using ZrO_2 balls in anhydrous ethanol for 24 h. After drying, the homogeneous mixture was calcined at 800 °C for 2 h. The powders obtained after the calcination process are compacted in the form of the discs using a hydraulic press. The pressed discs, were sintered in alumina crucibles, for 2 h, at temperature from 1200 °C. The preparation of the measuring electrodes for dielectric and piezoelectric properties requires the spreading of a very thin layer of the silver paste on both cylindrical sides of the samples and baked at 750 °C for 20 minutes. The application of a DC field 3.0 kV/mm for 10 minutes in a silicone oil bath at 90 ° C produces an electric polarization of the samples.

The Archimedes method is measured the densities of the sintered samples. X-ray diffraction (XRD) allowed characterizing the crystalline structures of the samples (Rigaku D/MAX 2400 diffractometer, Cu Kα). Raman spectroscopy studies were carried out at room temperature using a Renisaw Rm-1000 spectroscope.

After 24 h of polarization, the sintered ceramic samples are exposed to electrical properties measurements, using an AGILENT 4294A impedance analyzer. The dissipation factor and the dielectric constant were measured to 1 kHz. A quasi-static piezoelectric meter which ensures the measurements of the piezoelectric constants. Using the resonance-antiresonance method we obtain the electromechanical coupling factor [15].

Results and Discussion

Relative Densities and Phase Characterization

Among the factors influencing in a direct way on the properties of ceramics is the density factor. The dielectric and piezoelectric properties are strongly and positively related to the density of ceramics [16, 17]. Fig. 1 shows the effect of SFN content (wt.%) on the bulk density of sintered specimens. When the SFN content increases the relative density (i.e. the measured density divided by the theoretical density of PZT of 8.0 g/cm^3) of the ceramics also increases up to a value of x = 0.06 (99.75 % of the theoretical density), and then decreased for the ceramics with x > 0.06.

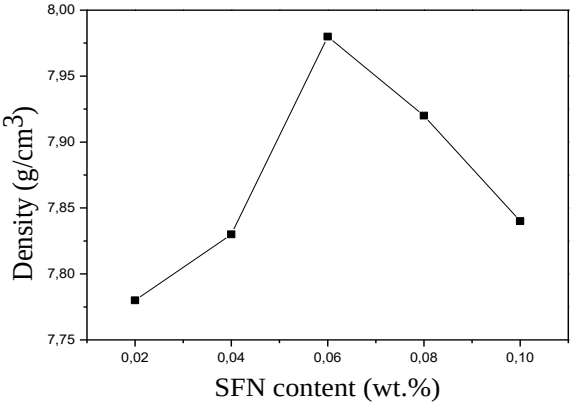

Fig. 1: Density of ceramics according to the SFN content.

Fig. 2 shows the XRD patterns for (1-x)PZT-xSFN with x = 0.02, 0.04, 0.06, 0.08 and 0.10 wt.% specimens at room temperature. It can be seen that a pure perovskite phase was obtained for all the compositions and all samples showed a single-phase perovskite structure without any traces of secondary phases, indicating that the Sr, Fe and Nb ions had been successfully diffused in to the lattice. For doped PZT samples (PZT-SFN), the tetragonal splitting of (200), (002) peaks was observed to 45°.

The difference in ionic size between Pb^{2+} and Sr^{2+} creates constraints in the crystal lattice of the samples, when the strontium concentration increases and by consequence a shift of peaks to higher angles is caused.

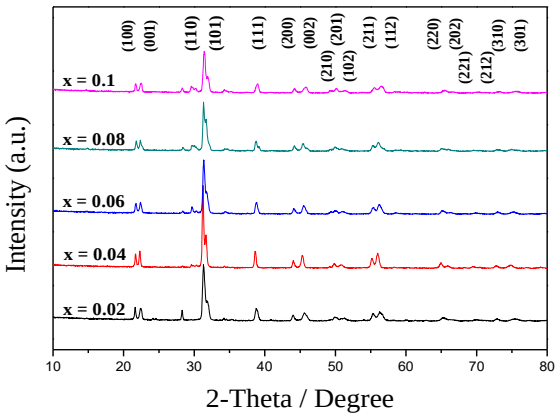

Fig. 2: XRD patterns of ceramics as a function of SFN content.

The Raman spectroscopy is sensitive to the symmetry of the crystalline structures and is thus used to study more in-depth the structure and the evolution of phase of our compounds.

The room temperature Raman spectra for (1-x)Pb($Zr_{0.53}$ $Ti_{0.47}$)O_3-xSr($Fe_{2/3}$, $Nb_{1/3}$)O_3 ceramics (x = 0.02, 0.04, 0.06, 0.08, and 0.10) during the frequency of 50-750 cm^{-1} are depicted in Fig. 3. The spectra show peaks around 200, 265, 328, 449, 558, 569 and 706 cm^{-1}, which corresponds to the Raman peaks PZT-SFN ceramic [18–21]. The Raman vibration mode of the PZT-SFN ceramic sintered samples is represented by specific and localized peaks, which confirms the purity of the samples. The E(2LO) and A_1(3TO) modes are related to Fe–O bonding vibration, O–B–O bending of the oxygen octahedron, respectively.

Fig. 3 (b) shows the Raman shifts of E + B_1, A_1 (3TO) and E (4LO) modes as a function of various SFN content (wt.%) of the (1-x) PZT-xSFN ceramic. In the wave number range of 550 to 700 cm^{-1}, it has been found that the Raman shift modes A_1(3TO) and E(4LO) are stable when the SFN content increases, where as the E+B1 mode is to take a lower wave number in the range of x = 0.02-0.06, and then pass to a higher wave number when X ≥ 0.06. These results show that the incorporation of the two dopants (Fe and Nb) within B-site of the perovskite structure causes a reduction in B-O binding energy when the SFN content (wt.%) increases to x = 0.06.

The Raman spectra confirm that the structure of (1-x) PZT-xSFN ceramics is tetragonal. The tetragonal phase and free of compositional inhomogeneity for all samples are confirmed by the Raman shifts and modes of Table-1.

Table-1: Peak positions of (1-x)PZT-xSFN for x = 0.02, 0.04, 0.06, 0.08 and 0.10 specimens in the range of 50-750 cm^{-1} [18–21].

Active mode	0.98PZT-0.02SFN	0.96PZT-0.04SFN	0.94PZT-0.06SFN	0.92PZT-0.08SFN	0.90PZT-0.10SFN	Vibration mode	Phase structure
A_1(1TO)	122.70	121.49	127.55	127.55	126.33	Cation-(BO_3) lattice modes	/
E(2TO)	199.04	200.25	196.61	200.25	200.25	BO_6 rotation	Tetragonal
Silent E+B_1	277.80	274.17	272.95	275.38	275.38	B-localized	Tetragonal or Rhombohedral
A_1(2TO)	328.69	328.69	327.48	328.69	328.69	BO_6 rotation	Tetragonal
E(2LO)	449.87	447.44	449.87	443.81	449.87	O-B-O bending	Tetragonal or Rhombohedral
E(3TO)	561.35	557.71	562.56	562.56	555.29	O-B-O bending	Tetragonal
A_1(3TO)	569.83	579.52	569.83	569.83	574.68	O-B-O bending	Tetragonal
E(4LO)	705.54	707.97	707.97	710.39	707.97	O-B-O bending	Tetragonal

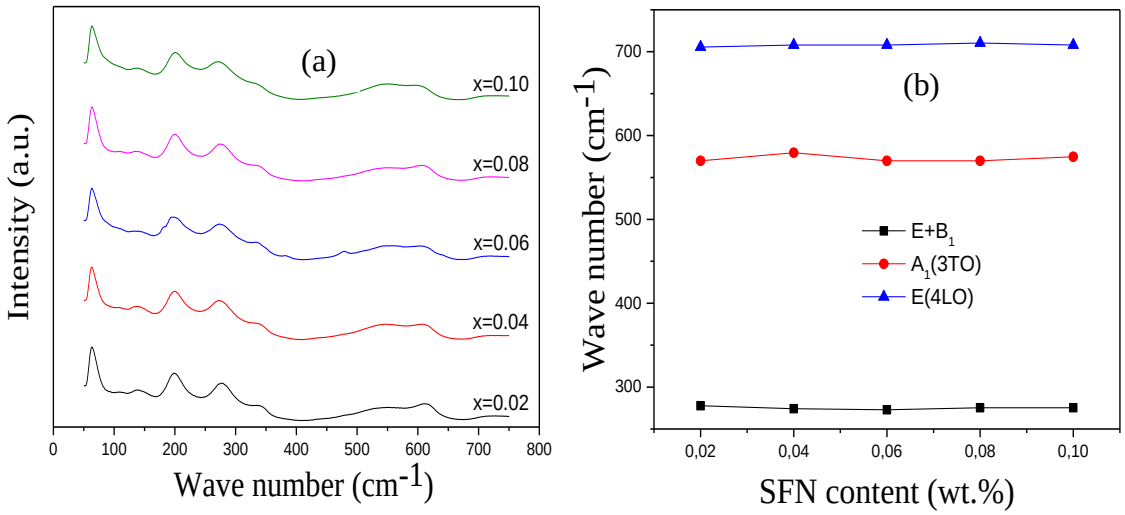

Fig. 3: Wave number (Raman shifts) of (a) various modes, and (b) E+B_1, A_1(3TO) and E(4LO) modes as a function of x content for (1-x)PZT-xSFN ceramics.

Dielectric and piezoelectric properties

Fig. 4 shows the evolution in the dissipation factor (tanδ) and dielectric constant (ε_r) characteristics of the SFN-doped systems. The two curves of Fig. 4, show inverse behavior with the increase in the SFN content. It has been found that ε_r increases and then decreases when the SFN content increases. The maximum ε_r value (1009) is obtained at 0.06 wt.% SFN content, which may be due to the high densification of the ceramics. However, the dielectric losses tanδ values of (1-x)PZT-xSFN reach a minimum value for 0.94PZT-0.06SFN (1.11%).

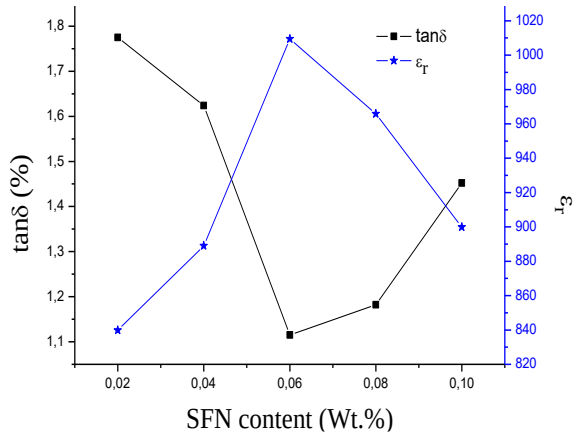

Fig. 4: Variation of tanδ and ε_r of ceramics as a function of SFN content.

Fig. 5(a, b) shows the electromechanical coupling factor (k_p), mechanical quality factor (Q_m), piezoelectric charge constant (d_{31}), and piezoelectric voltage constant (g_{31}), at room temperature of (1-x)PZT-xSFN ceramics with different SFN content. With increasing the amount of SFN addition, k_p, Q_m, d_{31}, and g_{31} increased at 0.06 wt.% SFN added specimen and then decreased.

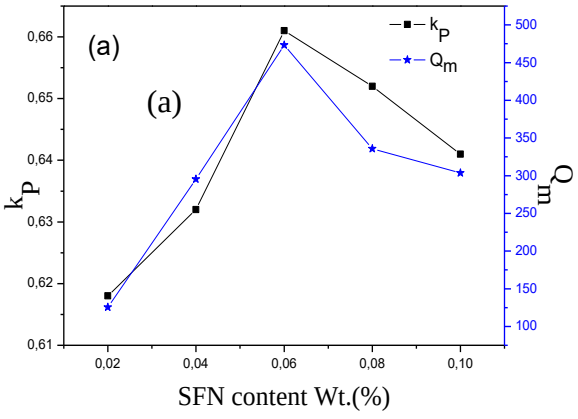

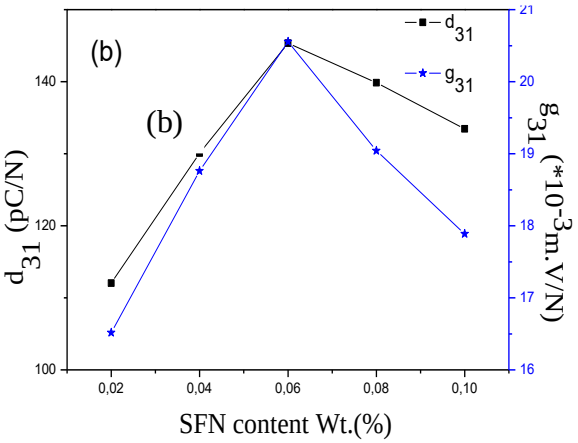

Fig. 5: SFN content Wt.(%) dependences of K_p, Q_m, d_{31}, and g_{31} for the (1-x)Pb($Zr_{0.53}$ $Ti_{0.47}$)O_3-xSr($Fe_{2/3}$, $Nb_{1/3}$)O_3 ceramics**.**

The two main factors that make electrical properties of ceramics better are the density and the vacancy effect [22]. During the polarization process, the two domains at 90° and 180° are oriented with a significant benefit for the domains at 90° because the domains at 180° are oriented in the polarization direction. The improvement of the electromechanical properties is made by a precise choice of doping level, the doping causes the appearance of the vacancies on the ceramics, by consequence these vacancies increases the rotation and favor the movement of domains with 90° [23]. The appearance of vacancies lead causes a distortion of the mesh and increases the movement of the domain walls [24]. The movement stability of the domain walls is related to an appropriate doping rate, caused by the reduction in grain size. Consequently, this reduction in grain size causes a strong interaction between the joints and the walls [25, 26].

Conclusions

In this study, a series of (1-x)Pb($Zr_{0.53}$ $Ti_{0.47}$)O_3-xSr($Fe_{2/3}$, $Nb_{1/3}$)O_3 ceramics were synthesized by conventional solid state process. The density, phase, dielectric and piezoelectric properties were systematically investigated. The X-ray diffraction (XRD) analyzes for all the samples synthesized in ceramics have a tetragonal crystalline structure. Raman spectroscopy confirms the presence of this tetragonal phase. The densification of ceramics is improved by the addition of modest amounts of SFN. Meanwhile, the piezoelectric properties are enhanced, especially the values of k_p, Q_m, d_{31} and g_{31}. As a result, the optimized values of K_p (0.661), Q_m(473), d_{31} (145 pC/N), g_{31} (0.020 mV/N), tanδ (0.011), ε_r (1009), are obtained for 0.06 Wt.% SFN.

References

1. B. Jaffe, W.J. Cook, H. Jaffe, *Piezoelectric ceramics*, Academic Press, New York-USA, (1971).
2. Y. Faheem, M. Shoaib, Sol–gel processing and characterization of phase-pure lead zirconate titanate nano-powders, *J. Am. Ceram. Soc.*, **89,** 2034 (2006).
3. S. Zhang, X. Wang, L. Li, Processing and characterization of lead zirconate titanate nano powders by a simple water-based sol–gel method, *J. Am. Ceram. Soc*., **95,** 3472 (2012).
4. B. Noheda, D. Cox, G. Shirane, J. Gonzalo, L. Cross, S. Park, A monoclinic ferroelectric phase in the $Pb(Zr_{1-x}Ti_x)O_3$ solid solution, *Appl. Phys. Lett.*, **74,** 2059 (1999).
5. S. Deluca, C. Galassi, G. Pezzotti, Investigation of local orientation and stress analysis of PZT-based materials using micro-probe polarized Raman spectroscopy, *J. Eur. Ceram. Soc.*, **26,** 2337 (2006).
6. J.H. Ma, X. Meng, J.L. Sun, T. Lin, F.W. Shi, J.H. Chu, Effect of annealing ambient on structure and ferroelectric properties of $Pb(Zr_{0.4}Ti_{0.6})O_3$ thin films on $LaNiO_3$ coated Si substrates, *Mat. Res. Bul.*, **140,** 221 (2005).
7. Y.J. Seo, J.S. Park, W.S. Lee, Chemical mechanical polishing of PZT thin films for FRAM applications, *Micr. Elect. Eng.*, **83,** 2238 (2006).
8. Z.A. Khorsand, W.H. ABDMajid, Effect of solvent on structure and optical properties of PZT nanoparticles prepared by sol–gel method, infrared region, *Ceram. Int.*, **37,** 753 (2011).
9. S. Uma, J. Philip, Induction of electro-activity in polyvinyl alcohol with addition of nanocrystalline PZT ceramic, *Indian. J. Pure. Appl. Phys.*, **51,** 717 (2013).
10. M. Goel, Recent developments in electroceramics: MEMS applications for energy and environment, *Ceram. Int.*, **30,** 1147 (2004).
11. R. Ragini, S.K. Mishra, D. Pandey, H. Lemmens, G.V. Tendeloo, Evidence for Another Low-Temperature Phase Transition in Tetragonal $Pb(Zr_xTi_{1-x})O_3$ (x=0.515, 0.520), *Phys. Rev. B.*, **64,** 054101 (2001).
12. R. Ragini, S. Ranjan, K. Mishra, D. Pandey, Room temperature structure of Pb $(Zr_xTi_{1-x})O_3$ around the morphotropic phase boundary region: A Rietveld study, *J. Appl. Phys.*, **92,** 3266 (2002).
13. M. Schwartz, *Smart Materials*, Vol. 2, John Wiley & Son. New York-USA, (2008).
14. W.Y. Choi, Eelectrical-properties of Sb-doped PZT films deposited by DC reactive sputtering using multi-targets, *Mater. Lett.*, **37,** 119 (1998).
15. L. Amarande, C. Miclea, C. Tanasoiu, Evaluation of the accuracy in determining the mechanical quality factor for piezoceramic resonators, *Ferroelectrics.*, **350,** 38 (2007).
16. S.Y. Chu, T.Y. Chen, I.T. Tsai, W. Water, Doping effects of Nb additives on the piezoelectric and dielectric properties of PZT ceramics and its application on SAW device, *Sens. Actuat. A. Phys.*, **113,** 198 (2004).
17. S.Y. Chu, Doping effects on the dielectric properties of low temperature sintered lead-based ceramics, *Mater. Res. Bull.*, **35,** 1067 (2000).
18. P. Cour, S.K. Pradhan, P. Kumar, S.K. Sinha, M. Kar, Enhanced ferroelectric and piezoelectric properties in La-modified PZT ceramics, *App. Phy. A.*, **122,** 591 (2016).
19. J. Wang, G. Wang, X. Chen, Z. Hu, H. Nie, F. Cao, X. Dong, An investigation on phase transition behaviors in MgO-doped $Pb_{0.99}(Zr_{0.95}Ti_{0.05})_{0.98}Nb_{0.02}O_3$ ferroelectric ceramics by Raman and dielectric measurements, *Mater. Sci. Engi. B.*, **193,** 170 (2015).
20. J. Zhu, C. Li, K. Jiang, P. Zhang, W.Y. Tong, A. Liu, W. Shi, Y. Liu, Y.P. Huang, W. Li, Z. Hu, Higher wavenumber shift of $Pb(Al_{1/2}Nb_{1/2})O_3$ substitution in relaxor ferroelectric $Pb(Zr_{0.52}Ti_{0.48})O_3$-$Pb(Zn_{1/3}Nb_{2/3})O_3$ ceramics, *Mater. Lett.* , **188,** 284 (2017).
21. A. Kumar, S.K. Mishra, Effects of Sr^{2+} substitution on the structural, dielectric, and piezoelectric properties of PZT-PMN ceramics, *Inter. J. Miner. Metall. Mate.*, **21,** 175 (2014).
22. F. Zhu, J. Qiu, H. Ji, K. Zhu, K. Wen, Comparative investigations on dielectric, piezoelectric properties and humidity resistance of PZT–SKN and PZT–SNN ceramics, *J. Mater. Sci. Mater. Electron.*, **26,** 2897 (2015).
23. K. Volkan, C. Ibrahim, T. Muharrem, Dielectric and piezoelectric properties of PZT ceramics doped with strontium and lanthanum, *Ceram. Int.*, **37,** 1265 (2011).
24. M.M.S. Pojucan, M.C.C. Santos, F.R. Pereira, M.A.S. Pinheiro, M.C. Andrade, Piezoelectric properties of pure and (Nb^{5+} + Fe^{3+}) doped PZT ceramics, *Ceram. Int.*, **36,** 1851 (2010).
25. N.J. Donnelly, T.R. Shrout, C.A. Randall, Addition of a Sr, K, Nb (SKN) combination to PZT (53/47) for high strain applications, *J. Am. Ceram. Soc.*, **90,** 490 (2007).
26. W.L. Zhang, R.E. Eitel, Low-temperature sintering and properties of 0.98PZT–0.02SKN ceramics with $LiBiO_2$ and CuO addition, *J. Am. Ceram. Soc.*, **94,** 3386 (2011).